Journal of proteome research

pubs.acs.org/jpr

Article

Identifying the Zoonotic Origin of SARS-CoV-2 by Modeling the Binding Affinity between the Spike Receptor-Binding Domain and Host ACE2

Xiaoqiang Huang, Chengxin Zhang, Robin Pearce, Gilbert S. Omenn, and Yang Zhang*

Cite This: *J. Proteome Res.* 2020, 19, 4844–4856

Read Online

ACCESS | Metrics & More | Article Recommendations | Supporting Information

ABSTRACT: Despite considerable research progress on SARS-CoV-2, the direct zoonotic origin (intermediate host) of the virus remains ambiguous. The most definitive approach to identify the intermediate host would be the detection of SARS-CoV-2-like coronaviruses in wild animals. However, due to the high number of animal species, it is not feasible to screen all the species in the laboratory. Given that binding to ACE2 proteins is the first step for the coronaviruses to invade host cells, we propose a computational pipeline to identify potential intermediate hosts of SARS-CoV-2 by modeling the binding affinity between the Spike receptor-binding domain (RBD) and host ACE2. Using this pipeline, we systematically examined 285 ACE2 variants from mammals, birds, fish, reptiles, and amphibians, and found that the binding energies calculated for the modeled Spike-RBD/ACE2 complex structures correlated closely with the effectiveness of animal infection as determined by multiple experimental data sets. Built on the optimized binding affinity cutoff, we suggest a set of 96 mammals, including 48 experimentally investigated ones, which are permissive to SARS-CoV-2, with candidates from primates, rodents, and carnivores at the highest risk of infection. Overall, this work not only suggests a limited range of potential intermediate SARS-CoV-2 hosts for further experimental investigation, but also, more importantly, it proposes a new structure-based approach to general zoonotic origin and susceptibility analyses that are critical for human infectious disease control and wildlife protection.

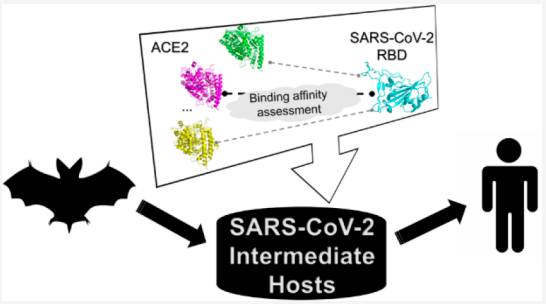

KEYWORDS: *SARS-CoV-2, zoonotic origin, intermediate host, binding affinity, EvoEF2 energy unit*

INTRODUCTION

Identification of the direct zoonotic origin (intermediate host) of severe acute respiratory syndrome coronavirus 2 (SARS-CoV-2) is important for combating the coronavirus disease 2019 (COVID-19) pandemic.[1,2] It has become well accepted that SARS-CoV-2 was likely to originate naturally from bats soon after its outbreak, built on the fact that SARS-CoV-2 shares a 96.2% nucleotide sequence identity with the bat coronavirus (CoV) RaTG13 isolated from *Rhinolophus affinis*[3] and that natural insertions were identified at the S1/S2 cleavage site of the Spike (S) protein of RmYN02-CoV isolated from *Rhinolophus malayanus*.[4] However, it remains unknown how the related CoV was transmitted from bats to humans.

In vitro experiments suggest that RaTG13 also binds to human angiotensin-converting enzyme 2 (hACE2) and can use hACE2 as an entry receptor;[5] thus, it could be possible that a progenitor of SARS-CoV-2, e.g., RaTG13 or RaTG13-like CoV, infected humans and evolved during human-to-human transmission.[6] However, recent experiments showed that the binding efficiency of RaTG13 to hACE2 is quite low,[7] probably due to the lack of critical hACE2-binding residues. Besides, no evidence has shown that RaTG13 can directly infect humans in nature.

It is widely believed that the novel CoV was transmitted from its natural host to humans via some intermediate host, during which a progenitor of SARS-CoV-2 acquired the critical ACE2 binding residues and/or furin cleavage site.[6] This point of view is supported in part by the fact that pangolin-CoV isolated from *Manis javanica* shares almost identical key ACE2-binding residues with SARS-CoV-2.[8−11] However, it is controversial whether pangolins are the intermediate host[9,10] or natural host,[8,11] or whether they are a host.[12,13] Phylogenetic analyses show that some pangolin-CoVs are genetically related to SARS-CoV-2 but do not sufficiently support SARS-CoV-2 emerging directly from these pangolin-CoVs.[14] Obtaining related viral sequences from animal sources would be the most definitive approach to identify the zoonotic origin of a virus.[6] For instance, the full-length genome sequences of viruses isolated from palm civets and camels

Special Issue: Human Proteome Project 2020

Received: September 15, 2020
Published: November 11, 2020

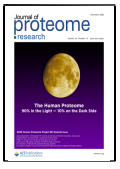

are 99.8% and 99.9% identical with human SARS-CoV and MERS-CoV,[15,16] respectively, thus consolidating that civets are the intermediate host for SARS-CoV and camels for MERS-CoV. In contrast, RaTG13 shares a genome identity of 96.2% with SARS-CoV-2,[3] and pangolin-CoVs only 85−93%,[8−11,13] which is not high enough to justify that bats or pangolins are a direct zoonotic host of SARS-CoV-2.

Early studies assumed that the outbreak of SARS-CoV-2 was associated with the Huanan Seafood and Wildlife Market, where one or more animals sold there may be the direct zoonotic source.[1,3,8] However, this point of view was challenged by the report that the first case of infection was suggested not to be related to the market.[17,18] Therefore, strategies to trace back the origin of SARS-CoV-2 should not be limited to the animals sold in the market, but should also include a wide range of wild animals outside the market. Theoretically, all kinds of animals that may have close contact with humans should be investigated, but this would be extremely laborious as well as time- and money-consuming.

ACE2 recognition by SARS-CoV-2 is an important determinant of viral infectivity and host range.[5,19] It has been reported that many animals can be infected by SARS-CoV-2.[20−28] In this work, we computationally examined the ACE2 usage of SARS-CoV-2 for 285 vertebrates by modeling the binding energy between the SARS-CoV-2 Spike receptor-binding domain (S-RBD) and host ACE2. The binding data correlate well with the reported experimental studies, perfectly distinguishing the effective ACE2 receptors from the less effective ones. Our results reveal that many mammals could serve as intermediate hosts of SARS-CoV-2. This work presents a fast and reliable computational approach to screen potential animal hosts for further experimental analyses.

MATERIALS AND METHODS

Collection and Examination of ACE2 Orthologs

A list of ACE2 orthologs from 318 vertebrate species was downloaded from the NCBI Web site (https://www.ncbi.nlm.nih.gov/gene/59272/ortholog/?scope=7742). Besides these, we also considered the ACE2 orthologs from three mammals that are not included in this list, namely, palm civets, raccoon dogs, and Chinese rufous horseshoe bats, as civets and raccoon dogs were suggested to be intermediate hosts of SARS-CoV.[15] Additionally, it was shown that the ACE2 proteins of civets and horseshoe bats can also be utilized by SARS-CoV-2 for viral entry in cell-level experiments.[3]

Among the 321 ACE2 orthologs, 30 sequences had one or more amino acids that were either nonstandard or incorrectly parsed, i.e., annotated as "X", and thus these ACE2 orthologs were excluded from the detailed analysis (Supplementary Table S1). Moreover, sequence alignment analysis (see below) showed that the ACE2 proteins of six species had five or more missing S-RBD binding residues (Supplementary Table S2), i.e., *Acanthisitta chloris* (protein accession ID: XP_009082150.1), *Apteryx mantelli mantelli* (XP_013805736.1), *Salmo salar* (XP_014062928.1), *Rhinopithecus bieti* (XP_017744069.1), *Leptonychotes weddellii* (XP_030886750.1), and *Petromyzon marinus* (XP_032835032.1). Subsequent binding analysis (see below) showed that these ACE2 receptors had a much higher binding energy (and thus a lower binding capability) than the others (Supplementary Table S2), partly because of the incomplete binding interface. Therefore, we cannot suggest whether these animals are susceptible to SARS-CoV-2 based on the defective information.

The remaining 285 ACE2 orthologs are summarized in Supplementary Table S3, including 134 mammals (*Mammalia*), 57 birds (*Aves*), 69 fish (*Actinopterygii* (66), *Chondrichthyes* (2), *and Sarcopterygii* (1)), 20 reptiles (*Reptilia*), and 5 amphibians (*Amphibia*). The protein ID, scientific classification (*Class* and *Species*), and common name are provided for easy retrieval.

Sequence Analyses

291 ACE2 sequences, including the six ACE2 proteins with missing S-RBD binding residues in Supplementary Table S2, were subjected to multiple sequence alignment (MSA) analysis using Clustal Omega[29] with default parameters. Pairwise sequence identities between the full-length sequence of hACE2 (accession ID: NP_001358344.1) and the other ACE2 sequences were calculated based on the MSAs. Besides the full-length sequence identities, the sequence identities for the 20 interface residues[30] and five critical S-RBD binding residues[31] were also calculated from the MSAs. The results for these three types of sequence identities are shown in Supplementary Table S4.

Structure Modeling

It should be mentioned that in reality, the ACE2 receptors of some animals may not bind to S-RBD. However, to quantitatively compare the capability of different ACE2 receptors to bind to S-RBD, we first constructed initial ACE2/S-RBD complex models through homology modeling, assuming that all the ACE2 receptors could bind to S-RBD, and then computed the binding energies between the two partners.

Pairwise sequence alignments between hACE2 and the other ACE2 orthologs were extracted from the MSAs and trimmed accordingly, as hACE2 was not full-length in the template complex (PDB ID: 6M0J).[30] The trimming should not affect binding analysis because it was shown that the protein−protein interface is unabridged in the experimentally determined hACE2/S-RBD complex structures.[5,30,32] We utilized Modeller v9.24[33] to build the initial putative complex models. Each model was first optimized with the variable target function method with conjugate gradients using parameters *library_schedule* = *autosched.slow* and *max_var_iterations* = *300*, and then refined using molecular dynamics with simulated annealing (SA) using parameter settings *md_level* = *refine.slow*. The whole cycle was repeated two times and was not stopped unless the objective function was $>1 \times 10^6$ (parameter settings: *repeat_optimization* = *2* and *max_molpdf* = *1e6*). For each ACE2/S-RBD pair, 100 initial Modeller complex models were constructed.

Binding Energy Calculation

Before binding energy calculation, each Modeller complex model was first repacked using FASPR[34] to eliminate rotamer outliers and then the interface residue side-chain conformations were thoroughly refined (both for ACE2 and S-RBD) using the EvoEF2 force field in conjunction with a simulated annealing Monte Carlo (SAMC) optimization procedure,[35,36] which was also utilized for anti-SARS-CoV-2 peptide design.[37] During the side-chain refinement process, both the ACE2 and S-RBD sequences were kept fixed, while the different rotameric side-chain conformations were sampled. Since a stochastic SAMC optimization procedure was used, obtaining the global

https://dx.doi.org/10.1021/acs.jproteome.0c00717
J. Proteome Res. 2020, 19, 4844−4856

energy minimum may not always be guaranteed. Therefore, the optimization of the interface residues was performed five times independently to generate five refined low-energy models. Hence, for each ACE2/S-RBD pair, 500 final models were generated and scored using EvoEF2.[35] The minimum binding interaction score achieved among all 500 complex models was regarded as the binding energy. The error bar of binding energy was estimated using bootstrapping. Specifically, in each step of bootstrapping, we performed a subsample with replacement for 500 data points from the original data set of 500 binding scores, and calculated the ensemble statistics (minimum in this case) for the subsampled data. The bootstrap steps were repeated for 1000 times to get 1000 minimum binding scores, and the standard deviation of these 1000 minimum values was taken as the length of error bar.

RESULTS

A Computational Pipeline for ACE2 Usage Analysis

Since SARS-CoV-2 utilizes ACE2 to invade host cells, ACE2 usage is considered to be an important determinant of infectivity and host range.[5,31] To examine the ACE2 usage by SARS-CoV-2, we developed a pipeline to model the binding energy between S-RBD and host ACE2 (Figure 1). We

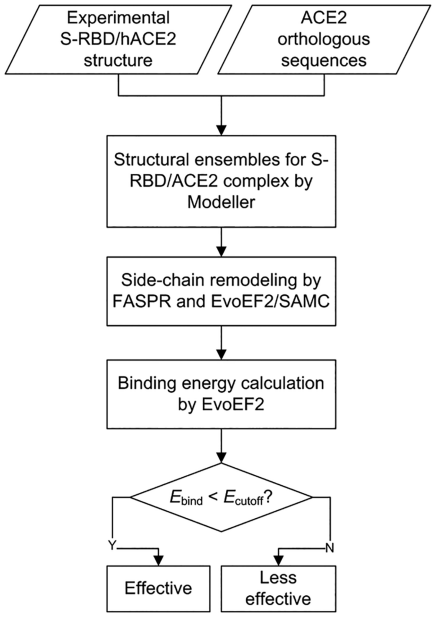

Figure 1. A computational pipeline for ACE2 usage analysis. 321 ACE2 orthologs were downloaded from NCBI. The crystal structure of the hACE2/S-RBD complex (PDB ID: 6M0J) was used as a template for homology modeling. For each ACE2/S-RBD pair, 100 initial Modeller complex models were constructed and repacked by FASPR, and then five models were generated by EvoEF2/SAMC remodeling for each FASPR model. The binding energy cutoff (E_{cutoff}) was set to −47 EvoEF2 energy units.

hypothesized that an effective ACE2 receptor should exhibit a low binding energy (or equivalently, a high affinity) while a poor receptor should have a high binding energy. A total of 321 ACE2 orthologs were collected from NCBI, and 285 of them were analyzed in detail after discarding 36 defective sequences (see Materials and Methods and Supplementary Tables S1, S2, and S3). Homologous structure models were built by Modeller[33] using the crystal structure of the hACE2/S-RBD complex (PDB ID: 6M0J)[30] as a template. Each initial complex model was then optimized using FASPR[34] and EvoEF2[35] to generate structure ensembles for binding energy calculation (see Materials and Methods). The ACE2 that achieved a binding energy below a given cutoff was suggested to be an effective receptor for SARS-CoV-2. During structure modeling and binding energy calculation, the N-glycosylation on ACE2 and S-RBD was ignored because current methods are not well adapted for modeling glycosylated amino acids.

Binding Energy Assessment and Correlation with Experimentally Determined ACE2 Usage Information

The length of the 285 ACE2 protein sequences ranged from 431 to 872 amino acids (Supplementary Table S3), where most ACE2 sequences were composed of about 800 amino acids (Supplementary Figure S1a). Five ACE2 sequences were partial (*Bison bison bison*, *Thamnophis sirtalis*, *Haliaeetus albicilla*, *Fulmarus glacialis*, and *Panthera tigris altaica*), but there were no missing interface residues according to sequence analysis. The ACE2 orthologs shared a sequence identity of ≥55% with hACE2 (Supplementary Figure S1b), indicating that the ACE2 proteins were conserved. Therefore, reliable structure models could be built by homology modeling. On the basis of the experimental structure of the hACE2/S-RBD complex, 20 residues (Q24, T27, F28, D30, K31, H34, E35, E37, D38, Y41, Q42, L79, M82, Y83, N330, K353, G354, D355, R357, and R393) were present at the interface of hACE2 within 4 Å of S-RBD.[30] Among the ACE2 orthologs, the sequence identities of the 20 interface residues to hACE2 ranged from 30% to 100% (Supplementary Figure S1c), while the sequence identities for the five key interface residues (K31, E35, D38, M82, and K353), which were regarded as important elements to determine host range,[31] varied from 0 to 100% (Supplementary Figure S1d).

The binding energy for the 285 ACE2 proteins ranged from −56.21 to −33.30 EvoEF2 energy units (EEU) (Supplementary Table S4), where a lower energy represents a stronger binding affinity, which may correspond to a higher susceptibility to SARS-CoV-2. However, it was unknown how trustable the energy values were, and it was not easy to understand whether or not an ACE2 was suggested to be an effective receptor. To address such issues, we compared the calculated binding energy with the experimental ACE2 usage data. Table 1 summarizes the reported infection cases in nature, and the infection studies in vivo and in vitro. Infections in nature represent those infection cases that take place naturally and have been confirmed by experiments such as quantitative real-time PCR.[38] In vivo infection means that the caged experimental animals can be infected by SARS-CoV-2,[20,24] while in vitro infection signifies that ACE2-expressing cells (e.g., HeLa cells transiently expressing ACE2) are permissive to SARS-CoV-2 infection.[3] Discrepancies may exist between in vivo, in vitro, and natural infections due to different experimental settings. For instance, it was reported that SARS-CoV-2 replicates poorly in dogs and pigs in vivo,[20] but it was shown that ACE2 of dogs and pigs could be effectively used for viral entry in vitro.[3,39] Moreover, pet dogs were reported to be infected naturally by their owners with COVID-19.[23] In this situation, an animal's ACE2 protein was regarded as an effective receptor to SARS-CoV-2 if any kind of experimental evidence held.

The calculated binding energy correlated well with the experimentally determined ACE2 usage data; the ACE2

https://dx.doi.org/10.1021/acs.jproteome.0c00717
J. Proteome Res. 2020, 19, 4844−4856

Table 1. The 59 Species Whose ACE2 Proteins Were Shown to Be Effective or Less Effective for SARS-CoV-2 Entry by Natural Infection and/or Experimental Studies[a]

index	animal name	binding energy (EEU)[b]	ACE2 usage[c]	experimental evidence
1	Sumatran orangutan	−56.21 ± 0.21	Y	in vitro[39]
2	Western gorilla	−55.84 ± 0.05	Y	in vitro[39]
3	Olive baboon	−55.77 ± 0.05	Y	in vitro[39]
4	Silvery gibbon	−55.73 ± 0.37	Y	in vitro[39]
5	Crab-eating macaque	−55.38 ± 0.04	Y	in vitro[39]
6	Gelada	−55.29 ± 0.09	Y	in vitro[39]
7	Rhesus macaque	−55.24 ± 0.53	Y	in vitro,[39] in vivo[27,28]
8	Human	−55.16 ± 0.10	Y	natural[2,40]
9	Golden snub-nosed monkey	−55.09 ± 0.50	Y	in vitro[39]
10	Chimpanzee	−54.97 ± 0.24	Y	in vitro[39]
11	Ugandan red colobus	−54.79 ± 0.13	Y	in vitro[39]
12	Golden hamster	−53.84 ± 0.05	Y	in vitro,[39] in vivo[25]
13	Chinese hamster	−53.77 ± 0.03	Y	in vitro[39]
14	Steller sea lion	−53.47 ± 0.18	Y	in vitro[39]
15	Horse	−52.95 ± 0.41	Y	in vitro[7,39]
16	Amur tiger	−52.93 ± 0.32	Y	natural[41]
17	Goat	−52.86 ± 0.06	Y	in vitro[7,39]
18	Rabbit	−52.84 ± 0.22	Y	in vitro[7,39]
19	Wild yak	−52.83 ± 0.06	Y	in vitro[39]
20	Puma	−52.79 ± 0.09	Y	in vitro[39]
21	Leopard	−52.74 ± 0.06	Y	in vitro[39]
22	Cattle	−52.71 ± 0.02	Y	in vitro[7,39]
23	Hawaiian monk seal	−52.56 ± 0.56	Y	in vitro[39]
24	Ferret	−52.55 ± 0.63	Y	in vitro,[39] in vivo[20,24]
25	California sea lion	−52.53 ± 0.80	Y	in vitro[39]
26	Water buffalo	−52.45 ± 0.05	Y	in vitro[39]
27	Lesser Egyptian jerboa	−52.44 ± 0.00	Y	in vitro[39]
28	Cat	−52.33 ± 0.20	Y	in vitro,[7,39] in vivo,[20] natural[21]
29	Canada lynx	−52.21 ± 1.16	Y	in vitro[39]
30	Giant panda	−52.21 ± 0.25	Y	in vitro[39]
31	White-footed mouse	−52.15 ± 0.11	Y	in vitro[39]
32	Sheep	−52.09 ± 0.59	Y	in vitro[7,39]
33	Beluga whale	−51.98 ± 0.11	Y	in vitro[39]
34	Sperm whale	−51.94 ± 0.40	Y	in vitro[39]
35	Polar bear	−51.93 ± 0.15	Y	in vitro[39]
36	Yangtze finless porpoise	−51.85 ± 0.21	Y	in vitro[39]
37	Malayan pangolin	−51.73 ± 0.35	Y	in vitro[7,39]
38	Red fox	−51.58 ± 0.18	Y	in vitro[39]
39	Dog	−51.38 ± 0.03	Y	in vitro,[39] in vivo,[20] natural[23]
40	Southern white rhinoceros	−51.08 ± 0.05	Y	in vitro[39]
41	Pig	−50.74 ± 0.14	Y	in vitro[3,7]
42	Arctic ground squirrel	−50.62 ± 0.22	Y	in vitro[39]
43	Chinese rufous horseshoe bat	−49.91 ± 0.15	Y	in vitro[39]
44	Bactrian camel	−49.88 ± 0.91	Y	in vitro[7,39]
45	Killer whale	−49.47 ± 0.03	Y	in vitro[39]
46	Long-finned pilot whale	−49.19 ± 0.10	Y	in vitro[39]
47	Atlantic bottle-nosed dolphin	−49.05 ± 0.11	Y	in vitro[39]
48	Yangtze river dolphin	−49.05 ± 0.02	Y	in vitro[39]
49	Masked palm civet	−47.97 ± 0.00	Y	in vitro[3,7]
50	Malayan tiger	n.d.	Y	natural[41]
51	African lion	n.d.	Y	natural[41]
52	Mink	n.d.	Y	natural[26]
53	Marmoset	−46.81 ± 0.13	N	in vitro,[39] in vivo[28]
54	Black-capped squirrel monkey	−46.71 ± 0.07	N	in vitro[39]
55	Tufted capuchin	−46.13 ± 0.28	N	in vitro[39]
56	Brown rat	−43.14 ± 0.15	N	in vitro[7,39]
57	House mouse	−42.62 ± 0.22	N	in vitro[7,39]
58	Duck	−42.54 ± 0.82	N	in vivo[20]
59	Chicken	−42.07 ± 1.65	N	in vitro,[7] in vivo[20]

[a]The table is organized by ranking the binding energy from low to high. [b]The binding energy was not calculated for Malayan tigers, lions, and minks because their ACE2 proteins were not included in the list of 321 ACE2 orthologs. EEU stands for EvoEF2 energy unit. [c]Y, effective ACE2 receptors; N, less effective ACE2 receptors. An ACE2 protein is classified as effective if at least one of the three kinds of experimental evidence holds.

proteins that can be more effectively used by SARS-CoV-2 achieved a relatively lower binding energy (Table 1). A binding energy cutoff of −47 EEU was able to discriminate the more efficient ACE2 receptors from the less efficient ones (Table 1), with the maximum Matthews correlation coefficient (MCC) of 1.0 (Supplementary Figure S2). Among all the experimental species, apes (Sumatran orangutan, western gorilla, silvery gibbon, and chimpanzee) and Old-World monkeys (olive baboon, crab-eating macaque, gelada, rhesus macaque, golden snub-nosed monkey, and Ugandan red colobus) and humans achieved the lowest binding energy ranging from −56.21 to −54.79 EEU (Table 1). Besides, a few rodents (golden hamster, Chinese hamster, jerboa, white-footed mouse, and Arctic ground squirrel) and carnivores (sea lion, tiger, puma, leopard, seal, ferret, dog, cat, lynx, and bear) also achieved a relatively low binding energy varying from −53.84 to −50.62 EEU (Table 1). Three New-World monkeys (marmoset, black-capped squirrel monkey, and tufted capuchin), rats, mice, ducks, and chickens achieved a higher binding energy score (> −47 EEU), consistent with the reports that these animals are less susceptible to SARS-CoV-2.[3,20,39,42]

Binding Energy-Based Intermediate Host Range Prediction

On the basis of the calculated binding energy and experimental data, we mapped the ACE2 usage effectiveness for each of the 285 species (Figure 2). Fish (including *Actinopterygii*, *Chondrichthyes*, and *Sarcopterygii*), amphibians, reptiles, and birds were predicted to have a relatively high binding energy (> −47 EEU), suggesting the ACE2 proteins of these species may be less permissive to SARS-CoV-2 binding. Mammals showed the broadest binding energy distribution, from −56.21 to −38.67 EEU (Figure 2 and Supplementary Table S4). 97 nonhuman mammals achieved a binding energy below −47

https://dx.doi.org/10.1021/acs.jproteome.0c00717
J. Proteome Res. 2020, 19, 4844−4856

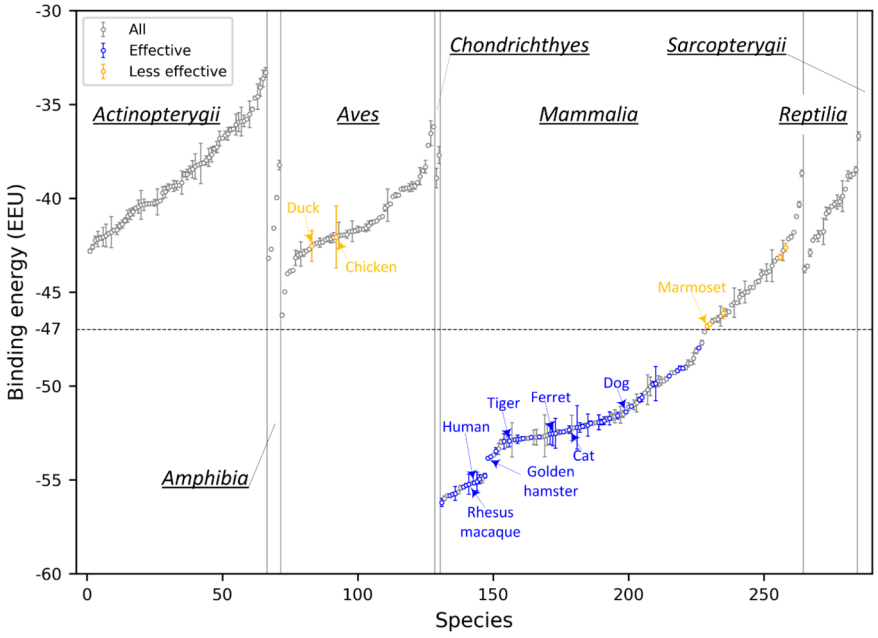

Figure 2. Mapping the calculated binding energy to 285 vertebrates. The ACE2 proteins are categorized by their animal Class (*Actinopterygii*, *Amphibia*, *Aves*, *Chondrichthyes*, *Mammalia*, *Reptilia*, and *Sarcopterygii*) and ranked by the binding energy from low to high in each Class. The ACE2 proteins that are experimentally shown to be effective or less effective to SARS-CoV-2 are shown in blue and orange circles, respectively, while the others are shown in gray circles. Susceptible and insusceptible animals are highlighted in blue and orange, respectively. The error bars were estimated via bootstrapping by subsampling with replacement for 500 data points from the original data set of 500 binding scores for each species; the bootstrap steps were repeated for 1000 times.

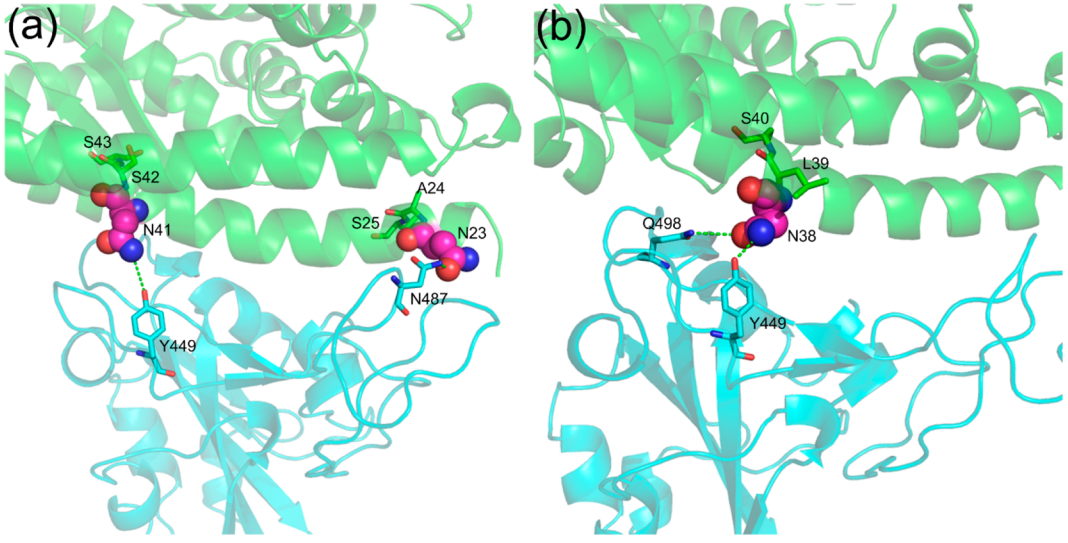

Figure 3. Putative N-glycosylation sites at the interface of two example ACE2/S-RBD complex structures. (a) Eurasian common shrew (*Sorex araneus*); and (b) Aardvark (*Orycteropus afer*). ACE2 and S-RBD are shown in green and cyan cartoons, respectively. The potential interface N-glycosylation motifs are shown with the asparagine residues highlighted in spheres.

EEU; that is, besides the experimentally validated species, another 49 species were also predicted to have an effective ACE2 receptor for SARS-CoV-2 (Figure 2 and Supplementary Table S4). These results suggest that mammals rather than other species are likely to be the main source of SARS-CoV-2 and hence they should be the major focus. This finding is also consistent with previous studies,[7,20,39,43−47] but a more quantitative measurement was given here. Our findings also refute isolated reports claiming that nonmammal vertebrates such as reptiles could be the intermediate host.[48,49]

The binding energy calculation did not consider the impact of possible N-glycosylation of ACE2 and Spike. Although no N-glycosylation site is present at the interface of the hACE2/S-RBD complex,[30] some ACE2 variants may have N-glycosylation sites at the interface region, which may prevent their binding to S-RBD due to steric hindrance. Thus, the analysis of interface N-glycosylation may help refine the list of effective ACE2 receptors classified by binding energy. N-glycosylation of asparagine occurs predominantly at the NX(T/S) motif, where X is any amino acid except proline. However, not all N-X-(T/S) sequons are glycosylated, so the

https://dx.doi.org/10.1021/acs.jproteome.0c00717
J. Proteome Res. 2020, 19, 4844−4856

Table 2. Forty-Eight Other Species Were Predicted to Have an Effective ACE2 Receptor Capable of S-RBD Binding[a]

index	species	animal name	binding energy (EEU)
1	*Pan paniscus*	Bonobo	−55.99 ± 0.12
2	*Nomascus leucogenys*	Northern white-cheeked gibbon	−55.84 ± 0.02
3	*Chlorocebus sabaeus*	Green monkey	−55.67 ± 0.04
4	*Macaca nemestrina*	Pig-tailed macaque	−55.42 ± 0.13
5	*Cercocebus atys*	Sooty mangabey	−55.19 ± 0.01
6	*Mandrillus leucophaeus*	Drill	−54.94 ± 0.22
7	*Nannospalax galili*	Northern israeli blind subterranean mole rat	−53.69 ± 0.18
8	*Propithecus coquereli*	Coquerel's sifaka	−53.35 ± 0.30
9	*Callorhinus ursinus*	Northern fur seal	−52.98 ± 0.14
10	*Equus przewalskii*	Mongolian wild horse	−52.95 ± 0.34
11	*Acinonyx jubatus*	Cheetah	−52.88 ± 0.92
12	*Heterocephalus glaber*	Naked mole-rat	−52.79 ± 0.04
13	*Bison bison bison*	Plains bison	−52.78 ± 0.08
14	*Mustela erminea*	Ermine	−52.74 ± 0.39
15	*Phoca vitulina*	Harbor seal	−52.73 ± 0.42
16	*Bos indicus x Bos taurus*	Hybrid cattle	−52.71 ± 0.02
17	*Lontra canadensis*	Northern American river otter	−52.66 ± 1.12
18	*Odobenus rosmarus divergens*	Walrus	−52.62 ± 0.53
19	*Bos indicus*	Zebu cattle	−52.47 ± 0.13
20	*Peromyscus maniculatus bairdii*	Deer mouse	−52.38 ± 0.07
21	*Odocoileus virginianus texanus*	White-tailed deer	−52.24 ± 0.67
22	*Fukomys damarensis*	Damaraland mole-rat	−52.22 ± 0.02
23	*Ursus arctos horribilis*	Grizzly bear	−52.13 ± 0.14
24	*Monodon monoceros*	Narwhal	−51.98 ± 0.07
25	*Phocoena sinus*	Vaquita	−51.95 ± 0.05
26	*Microtus ochrogaster*	Prairie vole	−51.76 ± 0.14
27	*Balaenoptera acutorostrata scammoni*	North pacific minke whale	−51.65 ± 0.19
28	*Marmota marmota*	Alpine marmot	−51.62 ± 0.35
29	*Ictidomys tridecemlineatus*	Thirteen-lined ground squirrel	−51.54 ± 0.44
30	*Marmota flaviventris*	Yellow-bellied marmot	−51.50 ± 0.19
31	*Canis lupus dingo*	Dingo	−51.11 ± 0.20
32	*Ochotona princeps*	American pika	−51.01 ± 0.26
33	*Rousettus aegyptiacus*	Egyptian rousette	−50.91 ± 0.48
34	*Lagenorhynchus obliquidens*	Pacific white-sided dolphin	−50.37 ± 0.07
35	*Nyctereutes procyonoides*	Raccoon dog	−50.20 ± 0.79
36	*Equus asinus*	Donkey	−50.02 ± 0.50
37	*Mirounga leonina*	Southern elephant seal	−49.75 ± 0.29
38	*Camelus dromedarius*	Arabian camel	−49.74 ± 0.22
39	*Phyllostomus discolor*	Pale spear-nosed bat	−49.73 ± 0.04
40	*Camelus ferus*	Wild bactrian camel	−49.63 ± 0.12
41	*Pteropus vampyrus*	Large flying fox	−49.29 ± 0.00
42	*Pteropus alecto*	Black flying fox	−49.29 ± 0.06
43	*Dipodomys ordii*	Ords kangaroo rat	−49.01 ± 0.13
44	*Loxodonta africana*	African savanna elephant	−48.80 ± 0.19
45	*Enhydra lutris kenyoni*	Sea otter	−48.53 ± 0.31
46	*Trichechus manatus latirostris*	Florida manatee	−48.13 ± 0.16
47	*Octodon degus*	Common degu	−47.70 ± 0.13
48	*Vicugna pacos*	Alpaca	−47.11 ± 0.07

[a]The table is organized by ranking the binding energy from low to high. The species in Table 1 were not included in this table. The binding energy cutoff (−47 EEU) was chosen by maximally discriminating the experimentally determined effective ACE2 receptors from the less effective ones.

motif alone may not be sufficient to discriminate between glycosylated and nonglycosylated asparagines. We tried three predictors, NGlycPred,[50] N-GlyDE,[51] and NetNGlyc (http://www.cbs.dtu.dk/services/NetNGlyc/), to predict N-glycosylation on hACE2. None of them could accurately predict all the experimentally identified N-glycosylation sites (Supplementary Table S5). All seven NX(T/S) motifs are glycosylated in the experimentally determined structure (PDB ID: 6M17),[52] indicating that ACE2 is highly N-glycosylated. To avoid the omission of potential glycosylation sites, we systematically examined all of the NX(S/T) motifs for the 285 ACE2 proteins and manually checked if any N-glycosylation sites were present at the interface.

Sixty-four out of the 285 ACE2 proteins were found to have one or more interface glycosylation sites, including 22 fish, one amphibian, 27 birds, seven mammals, and 7 reptiles (Supplementary Table S6). Since many mammals are likely susceptible to SARS-CoV-2 (Figure 2 and Supplementary Table S4), we examined the seven mammals and mapped the putative interface N-glycosylation sites into their structure models. Interestingly, none of the effective ACE2 receptors in Table 1 had an interface N-glycosylation site. The seven mammals were the Eurasian common shrew (*Sorex araneus*), small Madagascar hedgehog (*Echinops telfairi*), western European hedgehog (*Erinaceus europaeus*), aardvark (*Orycteropus afer*), big brown bat (*Eptesicus fuscus*), star-nosed mole (*Condylura cristata*), and greater horseshoe bat (*Rhinolophus ferrumequinum*), where their binding energies were −40.97, −44.99, −38.67, −48.79, −46.46, −45.56, and −44.47 EEU, respectively. Following the binding energy criterion, aardvark's ACE2 was predicted to be an effective receptor, but it may be ineffective due to glycosylation. The shrew had two interface glycosylation sites, N23 and N41, which form hydrogen bonds with N487 and Y449, respectively (Figure 3a); the aardvark had only one interface glycosylation site at N38, forming two hydrogen bonds with Y449 and Q498 (Figure 3b). Since these asparagine residues could form direct contact with S-RBD, their glycosylation may hinder the binding of the two proteins (i.e., ACE2 and Spike).

Following the binding energy calculation and interface N-glycosylation site analysis, 96 nonhuman ACE2 proteins were suggested to be effectively utilized by SARS-CoV-2; half of them have been confirmed by experiments (Table 1) and the other half are summarized in Table 2. Therefore, compared with the original list of 285 animals, our method considerably narrowed the host range. The predicted potential zoonotic animals are distributed widely, including pets, domestic, agricultural, and zoological animals that may have close contact with humans (Tables 1 and 2).

Case Studies

We then analyzed several ACE2 proteins to show molecular details about why they may or may not be effectively used by

https://dx.doi.org/10.1021/acs.jproteome.0c00717
J. Proteome Res. 2020, 19, 4844−4856

Table 3. Comparison of ACE2 Interface Residues and Binding Energy for Humans, Marmosets, Pangolins, and Turtles[a]

species	human (*H. sapiens*)	marmoset (*C. jacchus*)	pangolin (*M. javanica*)	turtle (*C. picta*)	turtle (*C. mydas*)	turtle (*P. sinensis*)
ACE2 interface residues	Q24	Q24	**E24**	**E24**	**E24**	**E24**
	T27	T27	T27	**N27**	**N27**	**N27**
	F28	F28	F28	F28	F28	F28
	D30	D30	**E30**	**S30**	**S30**	**S30**
	K31	K31	K31	**Q31**	**Q31**	**E31**
	H34	H34	**S34**	**V34**	**V34**	**V34**
	E35	E35	E35	**R35**	**R35**	**Q35**
	E37	E37	E37	E37	E37	E37
	D38	D38	**E38**	D38	D38	D38
	Y41	**H41**	Y41	Y41	Y41	Y41
	Q42	**E42**	Q42	**A42**	**A42**	**A42**
	L79	L79	**I79**	**N79**	**N79**	**N79**
	M82	**T82**	**N82**	**K82**	**K82**	**K82**
	Y83	Y83	Y83	Y83	Y83	Y83
	N330	N330	N330	N330	N330	N330
	K353	K353	K353	K353	K353	K353
	G354	**Q354**	**H354**	**K354**	**K354**	**K354**
	D355	D355	D355	D355	D355	D355
	R357	R357	R357	R357	R357	R357
	R359	R359	R359	R359	R359	R359
Binding energy (EEU)	−55.16	−46.81	−51.73	−43.61	−42.23	−40.68

[a]Five key residues are underlined. Amino acid mutations relative to hACE2 are shown in bold.

SARS-CoV-2 as an entry receptor. The first case is a New-World monkey, marmoset (*Callithrix jacchus*), which is of extremely low susceptibility to SARS-CoV-2 both in vivo and in vitro.[28,39] The marmoset achieved a high binding score of −46.81 EEU. Compared with hACE2, there were four residue substitutions in the marmoset ACE2, i.e., Y41H, Q42E, M82T, and G354Q (Table 3). In hACE2, Y41 could form hydrogen bonds with T500 in the RBD; Q42 could form a hydrogen bond with the carbonyl group of G446 and another hydrogen bond with Y449 where the NE2 atom of Q42 acts as the donor and the OH atom of Y449 as the acceptor (Figure 4a, left). The substitution of Y41 into histidine not only results in a reduced van der Waals packing energy but also disrupts the favorable hydrogen bond with T500; mutation of Q42 into glutamic acid destroys the two hydrogen bonds with G446 and Y449; moreover, the M82T substitution could lead to a reduced packing interaction with F486 due to the smaller side-chain (Figure 4a, right). The loss of three hydrogen bonds and the weakened van der Waals forces result in the poor binding energy. As reported, the double mutant H41Y/E42Q made the variant marmoset receptor more permissive to SARS-CoV-2 infection.[39] Besides the New-World monkeys, we found that the ACE2 proteins of four bats (i.e., *Eptesicus fuscus*, *Myotis brandtii*, *Myotis davidii*, and *Myotis lucifugus*) also have the Y41H/Q42E substitution (Supplementary Table S7); interestingly, they were also predicted to be less effective with a binding score of > −47 EEU.

The second case is Malayan pangolin (*Manis javanica*), which has been suggested as a potential intermediate host in a few studies.[9,10] Pangolin ACE2 shared an identity of 84.8%, 65%, and 60% with hACE2 for all, interface, and the key residues, respectively (Supplementary Table S4). Although pangolin ACE2 had seven residues mutated compared with hACE2, i.e., Q24E, D30E, H34S, D38E, L79I, M82N, and G354H, it still achieved a relatively low binding energy of −51.73 EEU (Table 3). In the hACE2/S-RBD complex, Q24 forms a hydrogen bond with N487, and D38 forms a hydrogen bond with Y449; D30 forms a salt bridge with K417; L79 and M82 form favorable van der Waals contacts with F486 (Figure 4b, left). In the pangolin-ACE2/S-RBD complex, favorable interactions are also extensively formed. E38 could form two hydrogen bonds with Q498 and Y449; E30 and E24 could form a hydrogen bond with K417 and N487, respectively; S34 could form a hydrogen bond with Y453 though it has a reduced van der Waals interaction due to the small size compared to H34; I79 and N82 could also form favorable packing interactions with F486 (Figure 4b, right). Therefore, although pangolin ACE2 achieved a higher binding score than hACE2, probably due to worse contacting geometries, the extensive favorable interactions demonstrate that pangolin ACE2 can still be an effective receptor to SARS-CoV-2. Thus, the binding analysis and molecular details supported Malayan pangolin as a possible intermediate host.

The third case is turtles (*Chrysemys picta*, *Chelonia mydas*, and *Pelodiscus sinensis*), which have been suggested as a potential intermediate host by Liu et al.[49] They argued that turtles have two important residues (Y41 and K353) in their ACE2 that are identical with those in hACE2 and that turtles in the markets were more common than pangolins.[49] Although it may be true that Y41 and K353 play an important role in binding S-RBD, it is, however, not a unique feature in the ACE2 of turtles and humans. As shown, many mammals have Y41 and K353 in their ACE2 proteins (Supplementary Table S7). Besides, the first reported case of infection was suggested not to be associated with the market.[17] Therefore, their rules for screening intermediate hosts were not persuasive. The ACE2 protein of these turtles has ten amino acid substitutions compared with hACE2 (Table 3). *C. picta* and *C. mydas* have identical interface residues in their ACE2 proteins. *P. sinensis* has two different interface residues (E31 and Q35) compared with *C. picta* and *C. mydas* (Table 3). In *C. picta*, only E24 could form a hydrogen bond with N487 (Figure 4c, right), while the other mutations resulted in a substantial loss of favorable hydrogen bonds and salt bridges compared with

https://dx.doi.org/10.1021/acs.jproteome.0c00717
J. Proteome Res. 2020, 19, 4844−4856

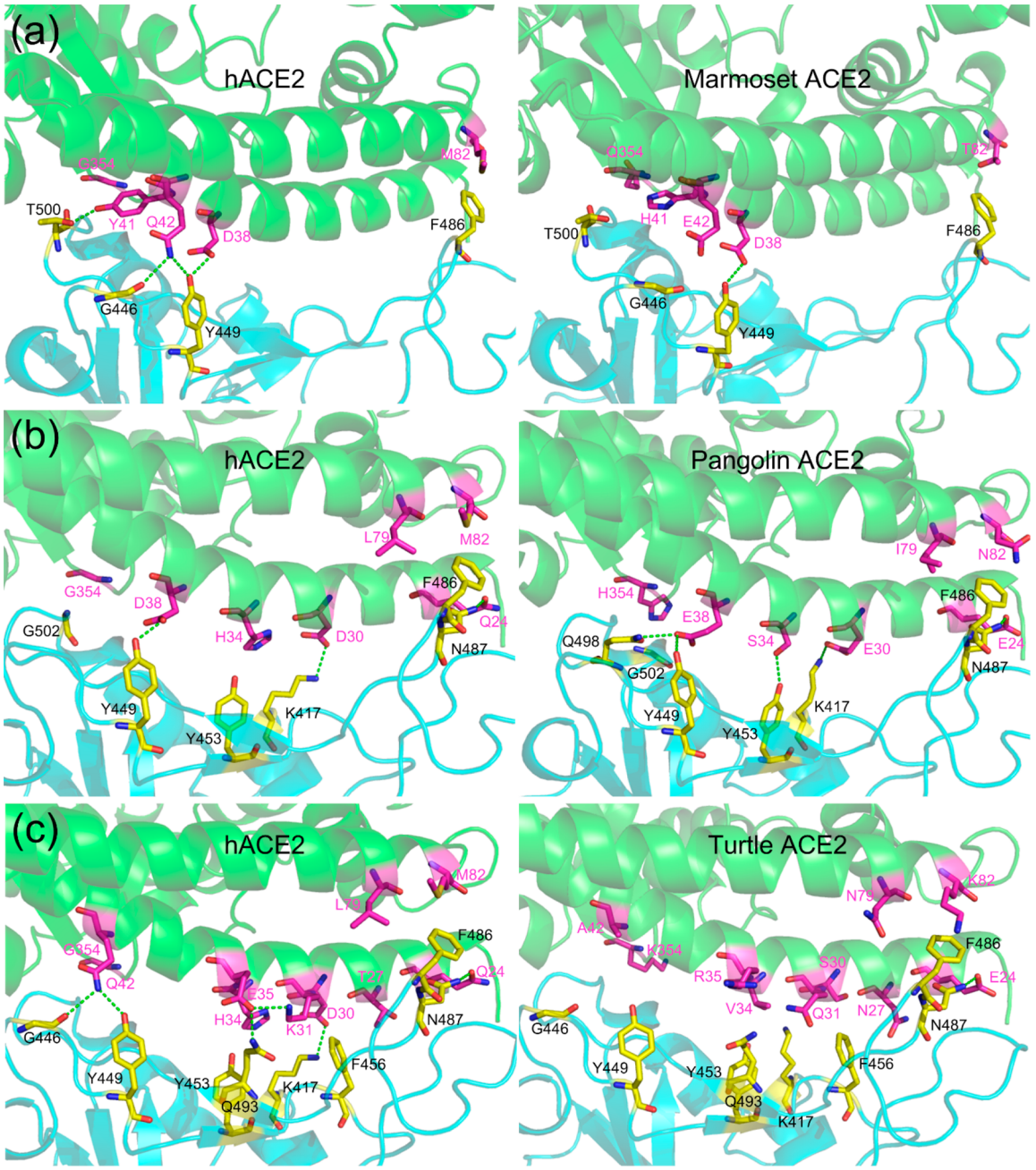

Figure 4. Comparison of the mutated interface between hACE2/S-RBD and animal-ACE2/S-RBD. (a) hACE2/S-RBD versus marmoset-ACE2/S-RBD; (b) hACE2/S-RBD versus pangolin-ACE2/S-RBD; and (c) hACE2/S-RBD versus turtle-ACE2/S-RBD. Residues in ACE2 and S-RBD are shown in magenta and yellow, respectively. Hydrogen bonds are shown in green dashed-lines.

those in the hACE2/S-RBD (Figure 4c, left). Expectedly, the three turtles (i.e., *C. picta*, *C. mydas*, and *P. sinensis*) achieved a poor binding score of −43.61, −42.23, and −40.68 EEU, respectively. Therefore, structure modeling did not support turtles as intermediate hosts.

DISCUSSION

As the COVID-19 pandemic continues, the direct zoonotic origin (intermediate host) of SARS-CoV-2 remains elusive. Many animals have been reported to be infected by SARS-CoV-2 in nature or the laboratory, suggesting a possibly wide host range for this novel coronavirus. Currently, the number of animals that have been experimentally tested is very small compared to the huge number of animal species. Previous studies suggested that receptor recognition is an important determinant of host range.[5,19,31] Therefore, we proposed a computational pipeline for identifying the intermediate hosts of SARS-CoV-2 by modeling the binding affinity between host ACE2 and the viral S-RBD. A recent study showed that, besides ACE2, alternative receptors such as ASGR1 or KREMEN1 may be sufficient to enable entry of SARS-CoV-2 into secretory cells and immune nonresident macrophages,[53] suggesting that these receptors may also play a role in SARS-CoV-2 susceptibility. However, in that study it was shown that, as the main receptor, ACE2 has a much higher binding capability for the extracellular domain of S protein than ASGR1 and KREMEN1; furthermore, ACE2 displayed a more significant correlation with virus susceptibility of ciliated cells

https://dx.doi.org/10.1021/acs.jproteome.0c00717
J. Proteome Res. 2020, 19, 4844−4856

when compared with the other two receptors.[53] At present, little is known about the atomic level protein−protein interactions between S and ASGR1 or KREMEN1, making it difficult to accurately model the binding affinity between the viral proteins and these receptors. Additionally, several in vitro and in vivo studies suggest that the susceptibility of different animals is mainly determined by the ACE2 receptor, as substituting the ACE2 alone is sufficient to enable SARS-CoV-2 infection of otherwise insusceptible cell lines[3,39] or animal models.[54,55] Therefore, the potential role of these alternative receptors on host determination was not considered in this work.

The Reasonability of Ignoring TMPRSS2

It has been shown that SARS-CoV-2 cell entry depends on ACE2 and the serine protease TMPRSS2.[56] However, we did not consider the role of TMPRSS2 for host prediction, due to the following reasons. First, TMPRSS2's role for priming Spike may be replaced by some other proteases like cathepsin B and L.[57] Second, different from ACE2 which is used as a binding receptor only, TMPRSS2 cleaves Spike through chemical catalysis. Thus, to quantify the impact of TMPRSS2, its catalytic activity for cleavage needs to be predicted; this is, however, an impossible task to achieve at present, as almost all protease cleavage predictors were trained to predict cleavage sites for one known protease of one species.[58] Third, TMPRSS2 proteases from different species may be similarly efficient. This is supported in part by the fact that wild-type mice are insusceptible to SARS-CoV-2, while transgenic mice that express hACE2 can be infected,[59] suggesting that mouse TMPRSS2 may be sufficiently efficient at cleaving Spike. Besides, a recent study showed that computational modeling failed to distinguish the binding capability of TMPRSS2 from different animals.[47] As a result, we believe that it may be reasonable to ignore TMPRSS2 for host prediction.

ACE2 Sequence Analysis Alone Is Not Accurate Enough for Host Identification

Built on the fact that hACE2 is highly susceptible to SARS-CoV-2, many previous studies only performed sequence analyses and used the sequence identity between animal ACE2 proteins and hACE2 to predict intermediate hosts,[44,49,60] as it was believed that the ACE2 proteins that are similar to hACE2 may also be susceptible.[6,31] We calculated the MCCs for distinguishing experimentally determined effective ACE2 receptors from the less effective ones listed in Table 1 using sequence identity. The maximum MCCs were 0.51, 0.73, and 0.53 with the optimum sequence identity cutoff of 66−78%, 61−65%, and ≤60% in terms of all, interface, and key residues, respectively (Supplementary Figure S3), which were much lower than that achieved by the classification via binding energy assessment (Supplementary Figure S2). Four New-World monkeys (*Sapajus apella*, *Aotus nancymaae*, *Saimiri boliviensis*, and *Callithrix jacchus*) share a relatively high sequence identity of >92%, 80%, and 80% with hACE2 in terms of all, interface, and key residues, respectively (Supplementary Tables S4 and S7). Following the optimum sequence identity cutoffs, the ACE2 proteins of these New-World monkeys were predicted to be very effective receptors. However, in vivo infection studies showed *C. jacchus* was not susceptible to SARS-CoV-2;[28] in vitro experiments also suggested that the ACE2 proteins of *S. apella*, *S. boliviensis*, and *C. jacchus* cannot be used by SARS-CoV-2.[39] In contrast, dogs, cats, and ferrets, which have a much lower sequence identity to hACE2 than the new-world monkeys (Supplementary Table S4), can be infected by SARS-CoV-2 in nature and/or in vivo.[20−24] These results suggest that an ACE2 protein with a higher sequence identity to hACE2 is not necessarily an effective receptor, whereas those with lower identities are not necessarily poor ones. Therefore, sequence identity between hACE2 and animal ACE2 may not be a good descriptor for host identification.

Binding Energy Is a Better Descriptor for Host Prediction

As indicated by the high MCC achieved (Supplementary Figure S2), structure-based binding energy assessment was more accurate than sequence identity for distinguishing experimentally confirmed species, provided that high-quality structure models were used. Critically, the structure models are highly likely to be very reliable given the high sequence similarity between hACE2 and the ACE2 orthologs and the application of advanced structure modeling tools.[33,34] Moreover, we argued that it is critical to model binding energy using structure ensembles rather than a single model. We found that the binding scores that were calculated for different models of the same ACE2/S-RBD complex fluctuated considerably (Supplementary Figure S4). The maximum MCC of the classification by the binding energy derived from the first model was only about 0.63 (Supplementary Figure S5), suggesting a single model was not sufficiently accurate for the classification even if a perfect scoring function was available. To circumvent the randomness of binding energy from a single model, we evaluated a large ensemble of structure models (e.g., 500 models in this work) for each complex and took the lowest binding score as the binding energy for ACE2 usage analysis. With a proper threshold (i.e., −47 EEU), the binding energy calculated in this manner correlated well with experimental data, perfectly distinguishing the experimentally determined effective ACE2 receptors from the less effective ones with a maximum MCC of 1.0 (Supplementary Figure S2). Nevertheless, it should be mentioned that biochemical and biophysical approaches, such as fluorescence resonance energy transfer experiments, are important for verifying the interaction between S and the ACE2 protein (or any other candidate receptors) from different species.

Identification and Screening of Potential Zoonotic Origins

The most definitive strategy to identify the direct zoonotic origins of SARS-CoV-2 is to isolate related viruses from animal sources.[6] Unlike SARS-CoV and MERS-CoV, whose direct zoonotic origins were identified to be civets[15] and camels,[16] respectively, soon after their outbreak, the clue for SARS-CoV-2 remains elusive as the first reported case of infection was suggested not to be associated with the Huanan Seafood and Wildlife Market.[17,18] As a result, a large number of animals have to be sampled to isolate viral strains that are highly similar to SARS-CoV-2 (e.g., >99% genome identity); this is a formidable task that would require extensive effort. In this regard, our work presents a fast, yet reliable approach for screening potential animals for further analysis. Our result suggests that many mammals are likely to be potential intermediate hosts of SARS-CoV-2, which is consistent with a few recent studies.[39,43,61] Here, the ACE2 proteins of 285 species were assessed because their sequences were of good quality. In reality, there are more animals whose ACE2 proteins have not been sequenced yet. Thus, although 96 mammals in this study were predicted to have an effective ACE2 receptor capable of binding SARS-CoV-2 Spike, it does

https://dx.doi.org/10.1021/acs.jproteome.0c00717
J. Proteome Res. 2020, 19, 4844−4856

not necessarily mean that the real intermediate host must be one of them. The list may be further screened by considering the living environment of animals. For instance, some mammals like whales and dolphins live in the water, and therefore the chance for them to transmit bat viruses to humans may be extremely low, considering that bats are terrestrial animals.

CONCLUSIONS

The direct zoonotic origin (intermediate host) of SARS-CoV-2 that caused the COVID-19 pandemic remains elusive. In this work, we developed a computational pipeline to facilitate the identification of potential intermediate hosts of SARS-CoV-2 by modeling the binding affinity between the SARS-CoV-2 Spike receptor-binding domain and the ACE2 protein of host animals. The effectiveness of this method was verified by its performance at perfectly distinguishing the experimentally determined effective ACE2 receptors from the less effective ones with a maximum Matthews correlation coefficient (MCC) of 1.0. Although the sequence identity-based descriptors have been widely used for predicting intermediate hosts, our results showed that their performance for discriminating between effective and less effective receptors was much worse than the binding-affinity-based approach proposed here by achieving a maximum MCC of 0.73. Our results reveal that SARS-CoV-2 may have a broad host range and a few mammals, especially some primates, rodents, and carnivores, rather than the nonmammal animals could be potential hosts of SARS-CoV-2. Additionally, as a supplementary to our previous pangolin coronavirus genome assembly study, the detailed structural modeling here also supports pangolins as a possible intermediate host with molecular-level insights. Since these animals are likely to be susceptible to SARS-CoV-2, continuous monitoring of viral circulation in them is very important for disease control and wildlife protection efforts.

ASSOCIATED CONTENT

Supporting Information

The Supporting Information is available free of charge at https://pubs.acs.org/doi/10.1021/acs.jproteome.0c00717.

Table S1: Thirty ACE2 proteins that were excluded from analysis due to inaccurate annotations in their sequences; Table S2: Six ACE2 proteins with five or more missing interface residues; Table S3: 285 ACE2 proteins used for detailed analysis in this work; Table S4: Binding energy and the three kinds of sequence identity for the 285 selected species; Table S5: Comparison of experimental and predicted N-glycosylation sites on hACE2; Table S6: Potential N-glycosylation sites in the 285 selected ACE2 proteins; Table S7: Comparison of the interface residues in the 285 ACE2 proteins; Figure S1: The distribution of protein length, and sequence identity for all, interface, and the five key residues for 285 ACE2 orthologs; Figure S2: Matthews correlation coefficient for classifying experimentally determined effective ACE2 receptors from the less effective ones by the binding energy calculated from 500 models; Figure S3: Matthews correlation coefficient for classifying experimentally determined effective ACE2 receptors from the less effective ones by sequence identity in terms of all, interface, and key residues; Figure S4: Binding score of 500 models for the hACE2/S-RBD complex; Figure S5: Matthews correlation coefficient for classifying experimentally determined effective ACE2 receptors from the less effective ones by the binding energy calculated from the first model (PDF)

AUTHOR INFORMATION

Corresponding Author

Yang Zhang − *Department of Computational Medicine and Bioinformatics and Department of Biological Chemistry, University of Michigan, Ann Arbor, Michigan 48109, United States;* orcid.org/0000-0002-2739-1916; Phone: +1 734 647 1549; Email: zhng@umich.edu; Fax: +1 734 615 6443

Authors

Xiaoqiang Huang − *Department of Computational Medicine and Bioinformatics, University of Michigan, Ann Arbor, Michigan 48109, United States;* orcid.org/0000-0002-1005-848X

Chengxin Zhang − *Department of Computational Medicine and Bioinformatics, University of Michigan, Ann Arbor, Michigan 48109, United States;* orcid.org/0000-0001-7290-1324

Robin Pearce − *Department of Computational Medicine and Bioinformatics, University of Michigan, Ann Arbor, Michigan 48109, United States*

Gilbert S. Omenn − *Department of Computational Medicine and Bioinformatics, University of Michigan, Ann Arbor, Michigan 48109, United States;* orcid.org/0000-0002-8976-6074

Complete contact information is available at: https://pubs.acs.org/10.1021/acs.jproteome.0c00717

Author Contributions

Y.Z. conceived and supervised the project; X.H. refined the structure models, performed sequence, structure, binding, and N-glycosylation analysis, and drafted the manuscript; C.Z. constructed the initial structure models; R.P. and G.S.O. participated in the discussion and edited the manuscript. All authors proofread and approved the final version of the manuscript.

Notes

The authors declare no competing financial interest.

ACKNOWLEDGMENTS

The work was supported by NIH grants (GM136422, S10OD026825, and AI134678 to Y.Z.; P30ES017885 and U24CA210967 to G.S.O.) and NSF grants (IIS1901191 and DBI2030790 to Y.Z.). The work used the XSEDE clusters,[62] which is supported by the National Science Foundation (ACI-1548562).

ABBREVIATIONS

ACE2, angiotensin-converting enzyme 2; COVID-19, coronavirus disease 2019; EEU, EvoEF2 energy unit; hACE2, human angiotensin-converting enzyme 2; MC, Monte Carlo; MCC, Matthews correlation coefficient; MSA, multiple sequence alignment; RBD, receptor-binding domain; S, Spike; SA,

https://dx.doi.org/10.1021/acs.jproteome.0c00717
J. Proteome Res. 2020, 19, 4844−4856

simulated annealing; SARS-CoV-2, severe acute respiratory syndrome coronavirus 2.

REFERENCES

(1) Wu, F.; Zhao, S.; Yu, B.; Chen, Y. M.; Wang, W.; Song, Z. G.; Hu, Y.; Tao, Z. W.; Tian, J. H.; Pei, Y. Y.; Yuan, M. L.; Zhang, Y. L.; Dai, F. H.; Liu, Y.; Wang, Q. M.; Zheng, J. J.; Xu, L.; Holmes, E. C.; Zhang, Y. Z. A new coronavirus associated with human respiratory disease in China. *Nature* **2020**, *579*, 265−269.

(2) Zhu, N.; Zhang, D.; Wang, W.; Li, X.; Yang, B.; Song, J.; Zhao, X.; Huang, B.; Shi, W.; Lu, R.; Niu, P.; Zhan, F.; Ma, X.; Wang, D.; Xu, W.; Wu, G.; Gao, G. F.; Tan, W. A Novel Coronavirus from Patients with Pneumonia in China, 2019. *N. Engl. J. Med.* **2020**, *382*, 727−733.

(3) Zhou, P.; Yang, X. L.; Wang, X. G.; Hu, B.; Zhang, L.; Zhang, W.; Si, H. R.; Zhu, Y.; Li, B.; Huang, C. L.; Chen, H. D.; Chen, J.; Luo, Y.; Guo, H.; Jiang, R. D.; Liu, M. Q.; Chen, Y.; Shen, X. R.; Wang, X.; Zheng, X. S.; Zhao, K.; Chen, Q. J.; Deng, F.; Liu, L. L.; Yan, B.; Zhan, F. X.; Wang, Y. Y.; Xiao, G. F.; Shi, Z. L. A pneumonia outbreak associated with a new coronavirus of probable bat origin. *Nature* **2020**, *579*, 270−273.

(4) Zhou, H.; Chen, X.; Hu, T.; Li, J.; Song, H.; Liu, Y.; Wang, P.; Liu, D.; Yang, J.; Holmes, E. C.; Hughes, A. C.; Bi, Y.; Shi, W. A Novel Bat Coronavirus Closely Related to SARS-CoV-2 Contains Natural Insertions at the S1/S2 Cleavage Site of the Spike Protein. *Curr. Biol.* **2020**, *30*, 2196−2203.

(5) Shang, J.; Ye, G.; Shi, K.; Wan, Y.; Luo, C.; Aihara, H.; Geng, Q.; Auerbach, A.; Li, F. Structural basis of receptor recognition by SARS-CoV-2. *Nature* **2020**, *581*, 221−224.

(6) Andersen, K. G.; Rambaut, A.; Lipkin, W. I.; Holmes, E. C.; Garry, R. F. The proximal origin of SARS-CoV-2. *Nat. Med.* **2020**, *26*, 450−452.

(7) Li, Y.; Wang, H.; Tang, X.; Ma, D.; Du, C.; Wang, Y.; Pan, H.; Zou, Q.; Zheng, J.; Xu, L.; Farzan, M.; Zhong, G. Potential host range of multiple SARS-like coronaviruses and an improved ACE2-Fc variant that is potent against both SARS-CoV-2 and SARS-CoV-1. *bioRxiv*, Apr 11, 2020, DOI: 10.1101/2020.04.10.032342 (accessed 2020-04-11).

(8) Lam, T. T.; Jia, N.; Zhang, Y. W.; Shum, M. H.; Jiang, J. F.; Zhu, H. C.; Tong, Y. G.; Shi, Y. X.; Ni, X. B.; Liao, Y. S.; Li, W. J.; Jiang, B. G.; Wei, W.; Yuan, T. T.; Zheng, K.; Cui, X. M.; Li, J.; Pei, G. Q.; Qiang, X.; Cheung, W. Y.; Li, L. F.; Sun, F. F.; Qin, S.; Huang, J. C.; Leung, G. M.; Holmes, E. C.; Hu, Y. L.; Guan, Y.; Cao, W. C. Identifying SARS-CoV-2-related coronaviruses in Malayan pangolins. *Nature* **2020**, *583*, 282−285.

(9) Xiao, K.; Zhai, J.; Feng, Y.; Zhou, N.; Zhang, X.; Zou, J. J.; Li, N.; Guo, Y.; Li, X.; Shen, X.; Zhang, Z.; Shu, F.; Huang, W.; Li, Y.; Zhang, Z.; Chen, R. A.; Wu, Y. J.; Peng, S. M.; Huang, M.; Xie, W. J.; Cai, Q. H.; Hou, F. H.; Chen, W.; Xiao, L.; Shen, Y. Isolation of SARS-CoV-2-related coronavirus from Malayan pangolins. *Nature* **2020**, *583*, 286−289.

(10) Zhang, C.; Zheng, W.; Huang, X.; Bell, E. W.; Zhou, X.; Zhang, Y. Protein Structure and Sequence Reanalysis of 2019-nCoV Genome Refutes Snakes as Its Intermediate Host and the Unique Similarity between Its Spike Protein Insertions and HIV-1. *J. Proteome Res.* **2020**, *19*, 1351−1360.

(11) Zhang, T.; Wu, Q.; Zhang, Z. Probable Pangolin Origin of SARS-CoV-2 Associated with the COVID-19 Outbreak. *Curr. Biol.* **2020**, *30*, 1346−1351.

(12) Li, X.; Zai, J.; Zhao, Q.; Nie, Q.; Li, Y.; Foley, B. T.; Chaillon, A. Evolutionary history, potential intermediate animal host, and cross-species analyses of SARS-CoV-2. *J. Med. Virol.* **2020**, *92*, 602−611.

(13) Liu, P.; Jiang, J. Z.; Wan, X. F.; Hua, Y.; Li, L.; Zhou, J.; Wang, X.; Hou, F.; Chen, J.; Zou, J.; Chen, J. Are pangolins the intermediate host of the 2019 novel coronavirus (SARS-CoV-2)? *PLoS Pathog.* **2020**, *16*, No. e1008421.

(14) Zhang, X.; Chen, X.; Zhang, Z.; Roy, A.; Shen, Y. Strategies to trace back the origin of COVID-19. *J. Infect.* **2020**, *80*, e39−e40.

(15) Guan, Y.; Zheng, B. J.; He, Y. Q.; Liu, X. L.; Zhuang, Z. X.; Cheung, C. L.; Luo, S. W.; Li, P. H.; Zhang, L. J.; Guan, Y. J.; Butt, K. M.; Wong, K. L.; Chan, K. W.; Lim, W.; Shortridge, K. F.; Yuen, K. Y.; Peiris, J. S.; Poon, L. L. Isolation and characterization of viruses related to the SARS coronavirus from animals in southern China. *Science* **2003**, *302*, 276−278.

(16) Hemida, M. G.; Chu, D. K.; Poon, L. L.; Perera, R. A.; Alhammadi, M. A.; Ng, H. Y.; Siu, L. Y.; Guan, Y.; Alnaeem, A.; Peiris, M. MERS coronavirus in dromedary camel herd, Saudi Arabia. *Emerging Infect. Dis.* **2014**, *20*, 1231−1234.

(17) Huang, C.; Wang, Y.; Li, X.; Ren, L.; Zhao, J.; Hu, Y.; Zhang, L.; Fan, G.; Xu, J.; Gu, X.; Cheng, Z.; Yu, T.; Xia, J.; Wei, Y.; Wu, W.; Xie, X.; Yin, W.; Li, H.; Liu, M.; Xiao, Y.; Gao, H.; Guo, L.; Xie, J.; Wang, G.; Jiang, R.; Gao, Z.; Jin, Q.; Wang, J.; Cao, B. Clinical features of patients infected with 2019 novel coronavirus in Wuhan. *Lancet* **2020**, *395*, 497−506.

(18) Cohen, J. Wuhan seafood market may not be source of novel virus spreading globally. *Science* **2020**, DOI: 10.1126/science.abb0611.

(19) Shang, J.; Wan, Y.; Luo, C.; Ye, G.; Geng, Q.; Auerbach, A.; Li, F. Cell entry mechanisms of SARS-CoV-2. *Proc. Natl. Acad. Sci. U. S. A.* **2020**, *117*, 11727−11734.

(20) Shi, J.; Wen, Z.; Zhong, G.; Yang, H.; Wang, C.; Huang, B.; Liu, R.; He, X.; Shuai, L.; Sun, Z.; Zhao, Y.; Liu, P.; Liang, L.; Cui, P.; Wang, J.; Zhang, X.; Guan, Y.; Tan, W.; Wu, G.; Chen, H.; Bu, Z. Susceptibility of ferrets, cats, dogs, and other domesticated animals to SARS-coronavirus 2. *Science* **2020**, *368*, 1016−1020.

(21) Halfmann, P. J.; Hatta, M.; Chiba, S.; Maemura, T.; Fan, S.; Takeda, M.; Kinoshita, N.; Hattori, S. I.; Sakai-Tagawa, Y.; Iwatsuki-Horimoto, K.; Imai, M.; Kawaoka, Y. Transmission of SARS-CoV-2 in Domestic Cats. *N. Engl. J. Med.* **2020**, *383*, 592−594.

(22) Goumenou, M.; Spandidos, D. A.; Tsatsakis, A. Possibility of transmission through dogs being a contributing factor to the extreme Covid19 outbreak in North Italy. *Mol. Med. Rep.* **2020**, *21*, 2293−2295.

(23) Sit, T. H. C.; Brackman, C. J.; Ip, S. M.; Tam, K. W. S.; Law, P. Y. T.; To, E. M. W.; Yu, V. Y. T.; Sims, L. D.; Tsang, D. N. C.; Chu, D. K. W.; Perera, R.; Poon, L. L. M.; Peiris, M. Infection of dogs with SARS-CoV-2. *Nature* **2020**, *586*, 776.

(24) Kim, Y. I.; Kim, S. G.; Kim, S. M.; Kim, E. H.; Park, S. J.; Yu, K. M.; Chang, J. H.; Kim, E. J.; Lee, S.; Casel, M. A. B.; Um, J.; Song, M. S.; Jeong, H. W.; Lai, V. D.; Kim, Y.; Chin, B. S.; Park, J. S.; Chung, K. H.; Foo, S. S.; Poo, H.; Mo, I. P.; Lee, O. J.; Webby, R. J.; Jung, J. U.; Choi, Y. K. Infection and Rapid Transmission of SARS-CoV-2 in Ferrets. *Cell Host Microbe* **2020**, *27*, 704−709.

(25) Sia, S. F.; Yan, L. M.; Chin, A. W. H.; Fung, K.; Choy, K. T.; Wong, A. Y. L.; Kaewpreedee, P.; Perera, R.; Poon, L. L. M.; Nicholls, J. M.; Peiris, M.; Yen, H. L. Pathogenesis and transmission of SARS-CoV-2 in golden hamsters. *Nature* **2020**, *583*, 834−838.

(26) Oreshkova, N.; Molenaar, R. J.; Vreman, S.; Harders, F.; Oude Munnink, B. B.; Hakze-van der Honing, R. W.; Gerhards, N.; Tolsma, P.; Bouwstra, R.; Sikkema, R. S.; Tacken, M. G.; de Rooij, M. M.; Weesendorp, E.; Engelsma, M. Y.; Bruschke, C. J.; Smit, L. A.; Koopmans, M.; van der Poel, W. H.; Stegeman, A. SARS-CoV-2 infection in farmed minks, the Netherlands, April and May 2020. *Euro Surveill.* **2020**, *25*, 2001005.

(27) Munster, V. J.; Feldmann, F.; Williamson, B. N.; van Doremalen, N.; Perez-Perez, L.; Schulz, J.; Meade-White, K.; Okumura, A.; Callison, J.; Brumbaugh, B.; Avanzato, V. A.; Rosenke, R.; Hanley, P. W.; Saturday, G.; Scott, D.; Fischer, E. R.; de Wit, E. Respiratory disease in rhesus macaques inoculated with SARS-CoV-2. *Nature* **2020**, *585*, 268.

(28) Lu, S.; Zhao, Y.; Yu, W.; Yang, Y.; Gao, J.; Wang, J.; Kuang, D.; Yang, M.; Yang, J.; Ma, C.; Xu, J.; Qian, X.; Li, H.; Zhao, S.; Li, J.; Wang, H.; Long, H.; Zhou, J.; Luo, F.; Ding, K.; Wu, D.; Zhang, Y.; Dong, Y.; Liu, Y.; Zheng, Y.; Lin, X.; Jiao, L.; Zheng, H.; Dai, Q.; Sun, Q.; Hu, Y.; Ke, C.; Liu, H.; Peng, X. Comparison of SARS-CoV-2 infections among 3 species of non-human primates. *bioRxiv*, Jul 17, 2020, DOI: 10.1101/2020.04.08.031807 (assessed 2020-07-17).

https://dx.doi.org/10.1021/acs.jproteome.0c00717
J. Proteome Res. 2020, 19, 4844−4856

(29) Sievers, F.; Wilm, A.; Dineen, D.; Gibson, T. J.; Karplus, K.; Li, W.; Lopez, R.; McWilliam, H.; Remmert, M.; Söding, J.; et al. Fast, scalable generation of high-quality protein multiple sequence alignments using Clustal Omega. *Mol. Syst. Biol.* **2011**, *7*, 539.
(30) Lan, J.; Ge, J.; Yu, J.; Shan, S.; Zhou, H.; Fan, S.; Zhang, Q.; Shi, X.; Wang, Q.; Zhang, L.; Wang, X. Structure of the SARS-CoV-2 spike receptor-binding domain bound to the ACE2 receptor. *Nature* **2020**, *581*, 215−220.
(31) Wan, Y.; Shang, J.; Graham, R.; Baric, R. S.; Li, F. Receptor Recognition by the Novel Coronavirus from Wuhan: an Analysis Based on Decade-Long Structural Studies of SARS Coronavirus. *J. Virol.* **2020**, *94*, e00127-20.
(32) Wang, Q.; Zhang, Y.; Wu, L.; Niu, S.; Song, C.; Zhang, Z.; Lu, G.; Qiao, C.; Hu, Y.; Yuen, K. Y.; Wang, Q.; Zhou, H.; Yan, J.; Qi, J. Structural and Functional Basis of SARS-CoV-2 Entry by Using Human ACE2. *Cell* **2020**, *181*, 894−904.
(33) Webb, B.; Sali, A. Protein structure modeling with MODELLER. In *Functional Genomics*; Springer, 2017; pp 39−54.
(34) Huang, X.; Pearce, R.; Zhang, Y. FASPR: an open-source tool for fast and accurate protein side-chain packing. *Bioinformatics* **2020**, *36*, 3758−3765.
(35) Huang, X.; Pearce, R.; Zhang, Y. EvoEF2: accurate and fast energy function for computational protein design. *Bioinformatics* **2020**, *36*, 1135−1142.
(36) Huang, X.; Pearce, R.; Zhang, Y. Toward the Accuracy and Speed of Protein Side-Chain Packing: A Systematic Study on Rotamer Libraries. *J. Chem. Inf. Model.* **2020**, *60*, 410−420.
(37) Huang, X.; Pearce, R.; Zhang, Y. *De novo* design of protein peptides to block association of the SARS-CoV-2 spike protein with human ACE2. *Aging* **2020**, *12*, 11263−11276.
(38) Corman, V. M.; Landt, O.; Kaiser, M.; Molenkamp, R.; Meijer, A.; Chu, D. K. W.; Bleicker, T.; Brunink, S.; Schneider, J.; Schmidt, M. L.; Mulders, D.; Haagmans, B. L.; van der Veer, B.; van den Brink, S.; Wijsman, L.; Goderski, G.; Romette, J. L.; Ellis, J.; Zambon, M.; Peiris, M.; Goossens, H.; Reusken, C.; Koopmans, M. P. G.; Drosten, C. Detection of 2019 novel coronavirus (2019-nCoV) by real-time RT-PCR. *Euro Surveill.* **2020**, DOI: 10.2807/1560-7917.ES.2020.25.3.2000045.
(39) Liu, Y.; Hu, G.; Wang, Y.; Zhao, X.; Ji, F.; Ren, W.; Gong, M.; Ju, X.; Li, C.; Hong, J.; Zhu, Y.; Cai, X.; Wu, J.; Lan, X.; Xie, Y.; Wang, X.; Yuan, Z.; Zhang, R.; Ding, Q. Functional and Genetic Analysis of Viral Receptor ACE2 Orthologs Reveals Broad Potential Host Range of SARS-CoV-2. *bioRxiv*, May 3, 2020, DOI: 10.1101/2020.04.22.046565 (assessed 2020-05-03) DOI: 10.1101/2020.04.22.046565.
(40) Holshue, M. L.; DeBolt, C.; Lindquist, S.; Lofy, K. H.; Wiesman, J.; Bruce, H.; Spitters, C.; Ericson, K.; Wilkerson, S.; Tural, A.; Diaz, G.; Cohn, A.; Fox, L.; Patel, A.; Gerber, S. I.; Kim, L.; Tong, S.; Lu, X.; Lindstrom, S.; Pallansch, M. A.; Weldon, W. C.; Biggs, H. M.; Uyeki, T. M.; Pillai, S. K. First Case of 2019 Novel Coronavirus in the United States. *N. Engl. J. Med.* **2020**, *382*, 929.
(41) Bartlett, S. L.; Diel, D. G.; Wang, L.; Zec, S.; Laverack, M.; Martins, M.; Caserta, L. C.; Killian, M. L.; Terio, K.; Olmstead, C.; Delaney, M. A.; Stokol, T.; Ivančić, M.; Jenkins-Moore, M.; Ingerman, K.; Teegan, T.; McCann, C.; Thomas, P.; McAloose, D.; Sykes, J. M.; Calle, P. P. SARS-CoV-2 Infection And Longitudinal Fecal Screening In Malayan Tigers (Panthera tigris jacksoni), Amur Tigers (Panthera tigris altaica), And African Lions (Panthera leo krugeri) At The Bronx Zoo, New York, USA. *bioRxiv*, Aug 14, 2020, DOI: 10.1101/2020.08.14.250928 (assessed 2020-08-14).
(42) Zhao, X.; Chen, D.; Szabla, R.; Zheng, M.; Li, G.; Du, P.; Zheng, S.; Li, X.; Song, C.; Li, R.; Guo, J.-T.; Junop, M.; Zeng, H.; Lin, H. Broad and differential animal ACE2 receptor usage by SARS-CoV-2. *J. Virol.* **2020**, DOI: 10.1128/JVI.00940-20.
(43) Damas, J.; Hughes, G. M.; Keough, K. C.; Painter, C. A.; Persky, N. S.; Corbo, M.; Hiller, M.; Koepfli, K.-P.; Pfenning, A. R.; Zhao, H.; Genereux, D. P.; Swofford, R.; Pollard, K. S.; Ryder, O. A.; Nweeia, M. T.; Lindblad-Toh, K.; Teeling, E. C.; Karlsson, E. K.; Lewin, H. A. Broad Host Range of SARS-CoV-2 Predicted by Comparative and Structural Analysis of ACE2 in Vertebrates. *bioRxiv*, Apr 18, 2020, DOI: 10.1101/2020.04.16.045302 (assessed 2020-04-18).
(44) Luan, J.; Lu, Y.; Jin, X.; Zhang, L. Spike protein recognition of mammalian ACE2 predicts the host range and an optimized ACE2 for SARS-CoV-2 infection. *Biochem. Biophys. Res. Commun.* **2020**, *526*, 165−169.
(45) Qiu, Y.; Zhao, Y. B.; Wang, Q.; Li, J. Y.; Zhou, Z. J.; Liao, C. H.; Ge, X. Y. Predicting the angiotensin converting enzyme 2 (ACE2) utilizing capability as the receptor of SARS-CoV-2. *Microbes Infect.* **2020**, *22*, 221−225.
(46) Zhai, X.; Sun, J.; Yan, Z.; Zhang, J.; Zhao, J.; Zhao, Z.; Gao, Q.; He, W. T.; Veit, M.; Su, S. Comparison of Severe Acute Respiratory Syndrome Coronavirus 2 Spike Protein Binding to ACE2 Receptors from Human, Pets, Farm Animals, and Putative Intermediate Hosts. *J. Virol.* **2020**, *94*, e00831-20.
(47) Lam, S. D.; Bordin, N.; Waman, V. P.; Scholes, H. M.; Ashford, P.; Sen, N.; van Dorp, L.; Rauer, C.; Dawson, N. L.; Pang, C. S. M.; Abbasian, M.; Sillitoe, I.; Edwards, S. J. L.; Fraternali, F.; Lees, J. G.; Santini, J. M.; Orengo, C. A. SARS-CoV-2 spike protein predicted to form stable complexes with host receptor protein orthologues from mammals, but not fish, birds or reptiles. *bioRxiv*, Aug 19, 2020, DOI: 10.1101/2020.05.01.072371 (assessed 2020-08-19).
(48) Ji, W.; Wang, W.; Zhao, X.; Zai, J.; Li, X. Cross-species transmission of the newly identified coronavirus 2019-nCoV. *J. Med. Virol.* **2020**, *92*, 433−440.
(49) Liu, Z.; Xiao, X.; Wei, X.; Li, J.; Yang, J.; Tan, H.; Zhu, J.; Zhang, Q.; Wu, J.; Liu, L. Composition and divergence of coronavirus spike proteins and host ACE2 receptors predict potential intermediate hosts of SARS-CoV-2. *J. Med. Virol.* **2020**, *92*, 595−601.
(50) Chuang, G.-Y.; Boyington, J. C.; Joyce, M. G.; Zhu, J.; Nabel, G. J.; Kwong, P. D.; Georgiev, I. Computational prediction of N-linked glycosylation incorporating structural properties and patterns. *Bioinformatics* **2012**, *28*, 2249−2255.
(51) Pitti, T.; Chen, C.-T.; Lin, H.-N.; Choong, W.-K.; Hsu, W.-L.; Sung, T.-Y. N-GlyDE: a two-stage N-linked glycosylation site prediction incorporating gapped dipeptides and pattern-based encoding. *Sci. Rep.* **2019**, *9*, 1−11.
(52) Yan, R.; Zhang, Y.; Li, Y.; Xia, L.; Guo, Y.; Zhou, Q. Structural basis for the recognition of SARS-CoV-2 by full-length human ACE2. *Science* **2020**, *367*, 1444−1448.
(53) Gu, Y.; Cao, J.; Zhang, X.; Gao, H.; Wang, Y.; Wang, J.; Zhang, J.; Shen, G.; Jiang, X.; Yang, J.; Zheng, X.; Xu, J.; Zhang, C. C.; Lan, F.; Qu, D.; Zhao, Y.; Xu, G.; Xie, Y.; Luo, M.; Lu, Z. Interaction network of SARS-CoV-2 with host receptome through spike protein. *bioRxiv*, Sep 13, 2020, DOI: 10.1101/2020.09.09.287508 (assessed 2020-09-13).
(54) Dinnon, K. H.; Leist, S. R.; Schäfer, A.; Edwards, C. E.; Martinez, D. R.; Montgomery, S. A.; West, A.; Yount, B. L.; Hou, Y. J.; Adams, L. E.; et al. A mouse-adapted model of SARS-CoV-2 to test COVID-19 countermeasures. *Nature* **2020**, *586*, 560−566.
(55) Goldman-Israelow, B.; Song, E.; Mao, T.; Lu, P.; Meir, A.; Liu, F.; Alfajaro, M. M.; Wei, J.; Dong, H.; Homer, R.; et al. Mouse model of SARS-CoV-2 reveals inflammatory role of type I interferon signaling. *J. Exp. Med.* **2020**, *217*, No. e20201241.
(56) Hoffmann, M.; Kleine-Weber, H.; Schroeder, S.; Kruger, N.; Herrler, T.; Erichsen, S.; Schiergens, T. S.; Herrler, G.; Wu, N. H.; Nitsche, A.; Muller, M. A.; Drosten, C.; Pohlmann, S. SARS-CoV-2 Cell Entry Depends on ACE2 and TMPRSS2 and Is Blocked by a Clinically Proven Protease Inhibitor. *Cell* **2020**, *181*, 271−280.
(57) Simmons, G.; Gosalia, D. N.; Rennekamp, A. J.; Reeves, J. D.; Diamond, S. L.; Bates, P. Inhibitors of cathepsin L prevent severe acute respiratory syndrome coronavirus entry. *Proc. Natl. Acad. Sci. U. S. A.* **2005**, *102*, 11876−11881.
(58) Fan, Y. X.; Zhang, Y.; Shen, H. B. LabCaS: labeling calpain substrate cleavage sites from amino acid sequence using conditional random fields. *Proteins: Struct., Funct., Genet.* **2013**, *81*, 622−634.
(59) Bao, L.; Deng, W.; Huang, B.; Gao, H.; Liu, J.; Ren, L.; Wei, Q.; Yu, P.; Xu, Y.; Qi, F.; Qu, Y.; Li, F.; Lv, Q.; Wang, W.; Xue, J.; Gong,

S.; Liu, M.; Wang, G.; Wang, S.; Song, Z.; Zhao, L.; Liu, P.; Zhao, L.; Ye, F.; Wang, H.; Zhou, W.; Zhu, N.; Zhen, W.; Yu, H.; Zhang, X.; Guo, L.; Chen, L.; Wang, C.; Wang, Y.; Wang, X.; Xiao, Y.; Sun, Q.; Liu, H.; Zhu, F.; Ma, C.; Yan, L.; Yang, M.; Han, J.; Xu, W.; Tan, W.; Peng, X.; Jin, Q.; Wu, G.; Qin, C. The pathogenicity of SARS-CoV-2 in hACE2 transgenic mice. *Nature* **2020**, *583*, 830−833.

(60) Luan, J.; Jin, X.; Lu, Y.; Zhang, L. SARS-CoV-2 spike protein favors ACE2 from Bovidae and Cricetidae. *J. Med. Virol.* **2020**, *92*, 1649.

(61) Li, F. Receptor recognition mechanisms of coronaviruses: a decade of structural studies. *J. Virol.* **2015**, *89*, 1954−1964.

(62) Towns, J.; Cockerill, T.; Dahan, M.; Foster, I.; Gaither, K.; Grimshaw, A.; Hazlewood, V.; Lathrop, S.; Lifka, D.; Peterson, G. D.; et al. XSEDE: accelerating scientific discovery. *Comput. Sci. Eng.* **2014**, *16*, 62−74.

https://dx.doi.org/10.1021/acs.jproteome.0c00717
J. Proteome Res. 2020, 19, 4844−4856